Infrared Studies Reveal Unique Vibrations Associated with the PGK−ATP−3-PG Ternary Complex†

Ellen M. White, Amanda R. Holland, and Gina MacDonald*

Department of Chemistry, James Madison University, Harrisonburg, Virginia 22807

Received August 23, 2007; Revised Manuscript Received November 9, 2007

ABSTRACT: Phosphoglycerate kinase (PGK) catalyzes a reversible phospho-transfer reaction between ATP and 3-phosphoglycerate (3-PG) that is thought to require a hinge-bending motion in the protein that brings two separate substrate-binding domains together. We have used difference infrared spectroscopy to better understand the conformational changes that are unique to the PGK−ATP−3-PG complex. Caged nucleotides (caged-ADP and caged-ATP) were used to initiate nucleotide binding to PGK or PGK−3-PG complexes. The difference spectra include those of PGK−ATP minus PGK, PGK−3-PG−ATP minus PGK−3-PG, PGK−3-PG−ADP minus PGK−3-PG, and PGK−ADP minus PGK. The resulting spectra were compared in attempts to identify bands associated with each PGK complex. In addition, complementary activity assays were performed in the presence of caged-nucleotides. While PGK activity decreased in the presence of caged-ADP, the activity was not influenced by the addition of caged-ATP. The activity assay results suggest that the caged-ADP may interact with PGK substrate binding site(s) and inhibit phospho-transfer. Therefore, additional difference infrared nucleotide exchange experiments were used to isolate the differences between ADP and ATP binding to PGK. Difference FTIR spectra obtained on PGK−nucleotide−3-PG complexes show distinct bands that may result from amino acid side chains as well as structural changes in the hinge region and/or increased interactions such as salt bridges forming between the two domains. The infrared data obtained on the active ternary complexes show evidence of changes in α-helix and *β*-structures as well as signals consistent with Arg, Asn, His, Lys, Asp, Glu, and additional side chains that are uniquely perturbed in the active ternary complex as compared to other PGK complexes.

The 45 kDa PGK[1] enzyme catalyzes the reversible phospho-transfer between 1,3-bisphosphoglycerate (1,3-bPG) and ADP to form 3-phosphoglycerate (3-PG) and ATP. PGK crystal structures show that PGK has two domains, the N-terminal domain that binds 3-PG and the C-terminal domain that binds MgATP or MgADP (*1*, *2*). Both domains of yeast PGK contain *β* strands that are surrounded by α-helices. The two domains are connected through a hinge region containing α, *β*, and irregular structures (*2*). It has been proposed that PGK must have a hinge-bending motion that brings the ATP closer to the 3-PG in order for the phospho-transfer reaction to occur (*1*). A hinge at *β*-strand L and additional salt bridges between domains are thought to be involved in domain closure (*3*−*7*). The general sequence and structure of PGK is highly conserved. To date, numerous crystal structures on different PGK complexes from a variety of sources have been obtained (for examples, see refs *1*−*3*, *6*−*14*). Many of these crystal structures are compared in Lee et al. (*7*). PGK crystals obtained in the presence of MgATP suggest multiple orientations of the terminal phosphate (*10*). Although the binding of two substrates was proposed to result in a closed conformation, many of the crystallized ternary complexes (PGK−ADP−3-PG or PGK−ATP-analogue−3-PG) retain open structures, as do many of the binary complexes (PGK−ADP and PGK−ATP) (*2*, *3*, *10*, *11*, *13*, *14*). The closed crystal structures that have been obtained are the *Thermotoga maritima* AMPPNP−3-PG complex (*6*) and the *Trypanosoma brucei* MgADP−3-PG complex (*8*, *9*). Studies that have compared many structures have shown that the species specific contacts between domains stabilize crystal conformations and help explain why domain closure is prevented in some PGK ternary complexes (*12*).

While crystal structures have not provided much evidence for a hinge-bending motion in yeast PGK, solution NMR studies suggest a PGK hinge-bending motion. The NMR studies also suggest that PGK may exist in multiple fluctuating conformations. Some of these conformations indicate greater flexibility and shorter distances between ATP and 3-PG for PGK in solution as compared to the PGK crystals (*15*−*17*). In addition to providing some evidence for domain closure, the NMR data have also shown that there is a primary anion binding site in the "basic patch" region of the N-terminal domain (*18*). The primary anion binding site shares two residues with the 3-PG binding site, His62 and

† This research was supported by The Henry Dreyfus Teacher-Scholar Awards Program and NSF-REU 0353807.

* To whom correspondence should be addressed. Phone: 540-568-6852. Fax: 540-568-7938. E-mail: macdongx@jmu.edu.

[1] Abbreviations: FTIR, Fourier transform infrared spectroscopy; HEPES, 4-(2-hydroxyethyl)piperazine-1-ethanesulfonic acid; PGK, phosphoglycerate kinase; 3-PG, 3-phosphoglyceric acid; 1,3-PG, 1,3-bisphosphoglycerate; ATP, adenosine 5′-triphosphate; ADP, adenosine 5′-diphosphate; caged-ATP or NPE-ATP, P^3-(1-(2-nitrophenyl)ethyl)-adenosine 5′-triphosphate; caged-ADP or NPE-ADP, P^2-(1-(2-nitrophenyl)ethyl)adenosine 5′-diphosphate; GAPDH, glyceraldehyde-3-phosphate dehydrogenase; NADH, reduced nicotinamide adenine dinucleotide; DTT, dithiothreitol.

10.1021/bi701723c CCC: $40.75
Published on Web 12/14/2007

Arg168, and has helped explain why high sulfate concentrations influence PGK structure and activity (*15*, *19*, *20*).

Additional evidence for domain closure in the ternary complexes was obtained from small-angle X-ray scattering experiments (SAXS) on human PGK (*5*). The results on the human PGK−MgATP−3-PG complexes also agree with previous studies on yeast complexes and favor a closed structure (*5*, *21*). Interestingly, the SAXS studies on human PGK−MgADP−3-PG complexes show some closure but not as much as the PGK−MgATP−3-PG structures (*5*). The SAXS results further solidify the assertion that the solution ternary complexes may be more compact than crystal complexes (*5*). Furthermore, protein unfolding studies on pig muscle and yeast PGK have indicated that the binding of either nucleotide (MgATP or MgADP) or 3-PG to yeast PGK stabilizes the overall structure (*4*). The unfolding studies also show that MgADP binding has a greater stabilization as compared to ATP binding, with the MgADP−PGK−3-PG ternary complexes being the most stable complexes studied (*4*). The increased stability of the ternary complexes may suggest additional interactions between side chains that are involved in domain closure (*4*).

The crystal structure of the yeast ternary complex shows an open conformation, while other SAXS and NMR studies suggest a closed structure. In order to obtain more information about the various PGK conformations, especially the active ternary complex, we have used difference Fourier transform infrared spectroscopy (FTIR). Difference FTIR has been successfully used to observe conformational changes in the protein backbone and side chains induced by substrate binding (for review, see refs *22*, *23*). This technique has allowed us to monitor protein structural changes induced by nucleotide binding to PGK in the presence and absence of 3-PG. In order to monitor these small structural changes, spectra must be collected before and after nucleotide binding. A caged-nucleotide is a convenient way to externally initiate substrate binding to PGK and generate high signal-to-noise difference infrared data. We used difference infrared spectroscopy to obtain information on each of the PGK complexes under the same conditions. The comparison of the data obtained on each of the complexes allows us to identify peaks specific to each of the ternary complexes and gain additional molecular level information about structural differences between the binary and ternary complexes. In addition, we have used nucleotide exchange experiments to isolate bands that arise from the differences associated with ADP and ATP binding to PGK and PGK−3-PG complexes. Some bands that were observed in the ternary complex difference spectra may be associated with the hinge-bending motion and the additional contacts between the C and N domains when PGK adopts a more closed conformation.

MATERIALS AND METHODS

Materials. Yeast phosphoglycerate kinase was purchased from Sigma-Aldrich and exchanged into buffer M that is composed of 20 mM Hepes, 1 mM $MgCl_2$, 1 mM dithiothreitol, and 1 mM EDTA, pH 7.5. Exchange was performed by centrifuging PGK in a Microsep 10k Omega centrifugal device from Pall Life Sciences with at least four dilution and concentration steps. The concentration of PGK was determined using the molar $\epsilon_{280} = 2.1400 \times 10^4\ M^{-1}\ cm^{-1}$ (*4*, *24*). The caged nucleotides, P^3-(1-(2-nitrophenyl)ethyl)-ester adenosine 5′-triphosphate (NPE-ATP) and P^2-(1-(2-nitrophenyl)ethyl)ester adenosine 5′-diphosphate (NPE-ADP), were purchased from Molecular Probes and dissolved in buffer M. Dithiothreitol, 3-phosphoglyceric acid (3-PG), reduced nicotinamide adenine dinucleotide (NADH), glyceraldehyde-3-phosphate dehydrogenase (GAPDH), ATP, and ADP were purchased from Sigma-Aldrich.

PGK Activity Assays. The rates for the reaction converting ATP and 3-PG to 1,3-bPG and ADP were determined using an enzyme-coupled assay previously described by Scopes (*25*) with several minor modifications. The assays were performed at room temperature in a Perkin-Elmer Lambda 2S UV/vis spectrometer. Each assay contained ATP with concentrations ranging from 0.025 to 0.25 mM, 0.16 mM NADH, 5 mM 3-PG, ∼1.7 μM GAPDH, and ∼1 nM PGK in buffer M. Additional assays were performed containing either 0.5 mM NPE-ATP or 0.5 mM NPE-ADP. In order to determine if PGK was still active in buffer salt concentrations that are estimated for partially dehydrated infrared sample conditions, additional activity assays were performed in a buffer containing 2000 mM Hepes, 100 mM $MgCl_2$, 100 mM dithiothreitol, and 100 mM EDTA, pH 7.5 (100× buffer M).

Preparation of IR Samples. The infrared samples contained approximately 10−25 nmol of protein, 80−170 nmol caged-nucleotide, and 10:1 ratio of dithiothreitol to caged-nucleotide in a final volume of approximately 100 μL. Some samples also contained a 5:1 ratio of 3-PG to PGK. PGK in buffer M (H_2O) was used for all infrared experiments. The protein samples were deposited on calcium fluoride windows and then partially dehydrated under a stream of nitrogen to decrease the strong water absorbance (*26*). Estimates obtained by weighing samples before and after dehydration suggest that the concentration of all components, including buffer salts, would increase by a factor of 100 after partial dehydration. A second calcium fluoride window was placed on top of the sample film (without a spacer) to form the infrared cell. The cell was placed in the Nicolet 560 Magna spectrometer equipped with a Mercury cadmium telluride/A liquid nitrogen-cooled detector. The resolution of the spectra was 4 cm^{-1}. Five hundred scans were coadded for each interferogram with the use of a mirror velocity of 1.8998 cm/s and a Happ-Genzel apodization function. Each spectrum took approximately 5 min to collect. The infrared samples were kept at −2 to −5 °C using a Fisher Scientific water bath and a Harrick temperature controller. A nitrogen laser (LSI Laser Science, Inc) was used to illuminate samples in the spectrometer and externally initiate photolysis of the caged-nucleotides.

Difference Infrared Spectra. Light-minus-dark infrared spectra were generated by taking a ratio of a single-beam spectrum taken after photolysis to a single-beam spectrum taken before photolysis (Figure 1). Multiple spectra were obtained before photolysis. A ratio was made of the spectra taken before photolysis to ensure that no significant spectral changes were observed before photolysis (Figure 1, dashed line). Three light-minus-dark infrared spectra obtained on each caged-nucleotide (caged-ATP or caged-ADP) in the absence of protein were averaged. Three light-minus-dark difference spectra on similar protein samples were averaged for each set of sample conditions. For direct comparison of the four different protein complexes, the averages of the

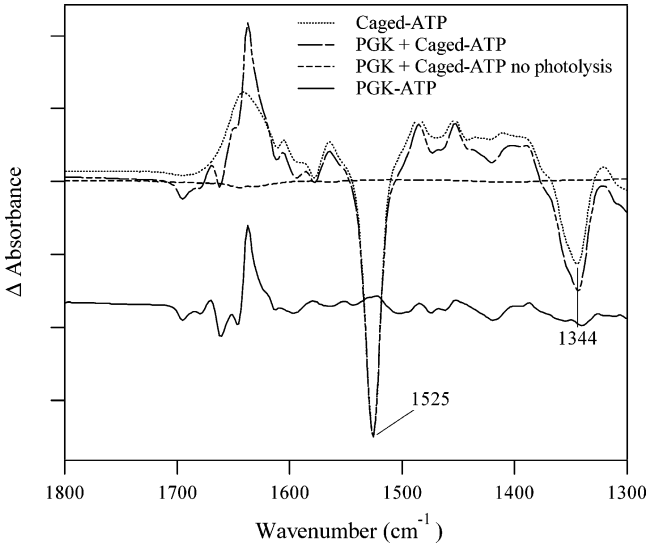

FIGURE 1: Spectra generated by taking a ratio of a spectrum taken after photolysis to a spectrum taken before photolysis on samples containing caged-ATP (dotted line, top) and caged-ATP and PGK (long dashed line, top). A control difference spectrum (dashed line) was obtained on the sample containing caged-ATP and PGK by taking a ratio of two spectra taken before photolysis. The resulting difference spectrum PGK−ATP minus PGK (solid line) obtained after normalization of caged-ATP spectrum (dotted line) was subtracted from the PGK + caged-ATP (long dashed line) spectrum. Tick marks correspond to 5×10^{-3} absorbance units.

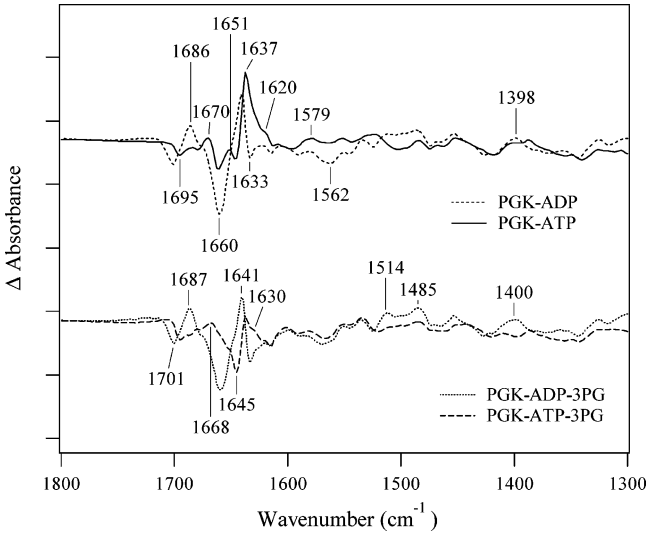

FIGURE 2: Difference spectra generated by subtracting a normalized light minus dark difference spectrum of caged-nucleotide (average of spectra obtained in the absence of protein) from a light-minus-dark averaged spectrum containing protein and caged-nucleotide. The 1800−1300 cm^{-1} region of the difference spectra shown are for the following: PGK−ATP minus PGK, PGK−ADP minus PGK, PGK−ADP−3-PG minus PGK−3-PG, and PGK−ATP−3-PG minus PGK−3-PG. Tick marks correspond to 5×10^{-3} absorbance units.

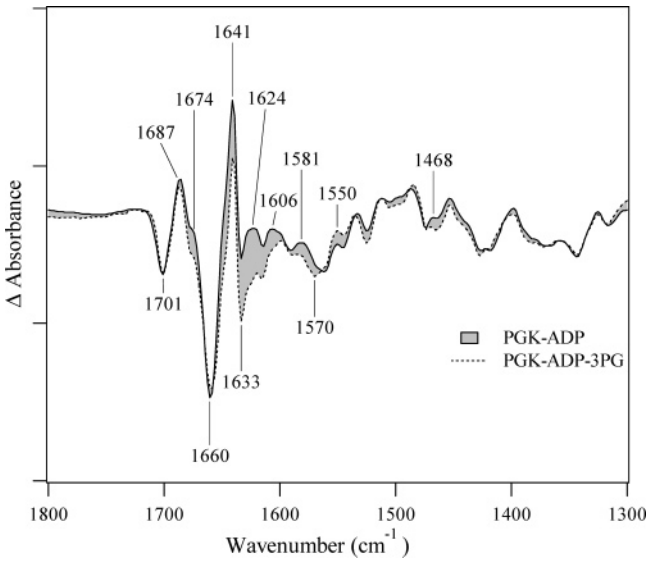

FIGURE 3: Difference spectra generated by subtracting a normalized light-minus-dark difference spectrum of caged-nucleotide (average of spectra obtained in the absence of protein) from a light-minus-dark averaged spectrum containing protein and caged-nucleotide (same as shown in Figure 2). The 1800−1300 cm^{-1} region of the difference spectra shown are for the following: PGK−ADP minus PGK (solid line) and PGK−ADP−3-PG minus PGK−3-PG (dashed line). The shaded areas highlight the differences between the two spectra. Tick marks correspond to 5×10^{-3} absorbance units.

difference spectra were then normalized for protein content using the amide I (∼1650 cm^{-1}) vibration of the corresponding averaged absorbance spectra. Normalization of spectra was also obtained using the amide II (∼1550 cm^{-1}) vibration and spectra were found to be nearly identical to those presented in this paper (data not shown). Difference infrared spectra were generated by subtracting the averaged, weighted-difference infrared spectrum of a sample containing only caged-nucleotide (Figure 1, dotted line) from an averaged difference spectrum containing caged-nucleotide and protein (Figure 1, long dashed line). The strong 1525 and 1344 cm^{-1} bands associated with asymmetric and symmetric NO_2 vibrational peaks from the nitrophenyl cage were used to normalize the amount of nucleotide released between samples (*27*). Difference data were obtained using caged-ADP and caged-ATP to generate PGK−ATP minus PGK and PGK−ADP minus PGK difference spectra. In addition, data were also collected for samples that contained PGK−3-PG and caged-nucleotides in order to obtain PGK−ATP−3-PG minus PGK−3-PG and PGK−ADP−3-PG minus PGK−3-PG data. Direct comparison of the difference spectra shown in Figures 2−4 can be performed.

PGK samples containing ADP or ADP and 3-PG with caged-ATP were used to investigate the effects of nucleotide exchange on PGK complexes. Samples contained 10−15 nmol of PGK, 140 nmol of caged-ATP, 15 nmol of ADP, and 1.5 μmol of DTT. Some samples also contained 15 nmol of 3-PG. For direct comparison of the two different protein complexes (PGK−ADP and PGK−ADP−3-PG), the light-minus-dark averages were then normalized for protein content using the amide I (∼1650 cm^{-1}) vibration of the corresponding averaged absorbance spectra. Three light-minus-dark difference spectra on similar samples were averaged for each set of sample conditions, and subtractions to remove contributions from the photolytic release of the cage were performed as described above in order to yield the PGK−ATP minus PGK−ADP and PGK−ATP−3-PG minus PGK−ADP−3-PG difference spectra shown in Figure 5.

RESULTS AND DISCUSSION

Enzyme Activity Assays. An enzyme-coupled activity assay was used to monitor the activity of PGK. The assay couples the formation of every 1,3-bPG to the oxidation of one

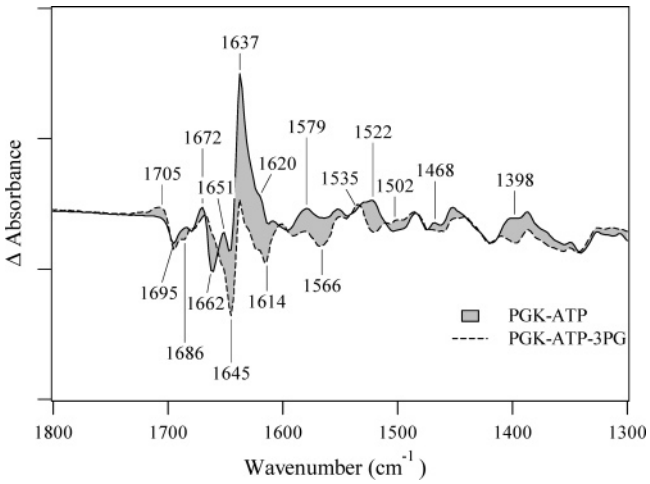

FIGURE 4: Difference spectra generated by subtracting a normalized light-minus-dark difference spectrum of caged-nucleotide (average of spectra obtained in the absence of protein) from a light-minus-dark averaged spectrum containing protein and caged-nucleotide (same as shown in Figure 2). The 1800−1300 cm^{-1} region of the difference spectra shown are for the following: PGK−ATP minus PGK (solid line) and PGK−ATP−3-PG minus PGK−3-PG (dashed line). The shaded areas highlight the differences between the two spectra. Tick marks correspond to 5×10^{-3} absorbance units.

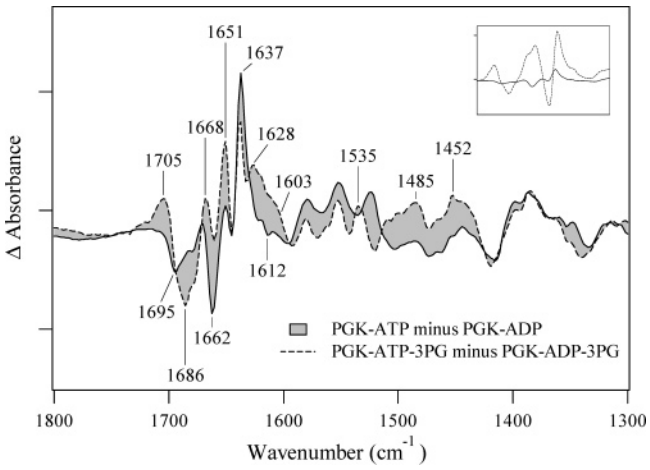

FIGURE 5: Difference spectra generated by subtracting a normalized light-minus-dark difference spectrum of caged-ATP (average of spectra obtained in the absence of protein) from a light-minus-dark averaged spectrum containing PGK−ADP (solid line) or PGK−ADP−3-PG (dashed line) and caged-ATP. The shaded areas highlight the differences between the two spectra. Tick marks correspond to 1×10^{-3} absorbance units. The inset shows an overlay of the PGK−ATP minus PGK−ADP exchange spectrum (solid line) with a spectrum obtained by subtracting PGK−ADP (Figure 2, dashed line top) from PGK−ATP spectrum (Figure 2, solid line top). The *x*-axis for the inset ranges from 1720 to 1580 cm^{-1} and the tick marks for the inset correspond to 5×10^{-3} absorbance units.

NADH. The rates of PGK activity were calculated from the change in NADH concentration over time. Three samples were assayed and averaged for each rate presented in Table 1. Caged-ATP (0.5 mM) was added to the assays at each concentration of ATP. PGK activities calculated from assays performed in the presence and absence of caged-ATP were very similar to those obtained in the absence of any caged-nucleotides. Therefore, we suggest that the presence of caged-ATP is not significantly preventing ATP and/or 3-PG from binding under the conditions used for the activity assays. However, activity assays performed in the presence of caged-ADP (0.5 mM) resulted in decreased activity at all concentrations of ATP tested. Inspection of the crystal structure indicates that the interaction of caged-ADP with the nucleotide binding site may position the cage in such a manner that the 3-PG is unable to successfully bind to PGK (*2*). Equilibrium dialysis experiments have also suggested that MgADP binding is competitive with both MgATP and 3-PG binding (*28*). It should be noted that we are not able to perform activity assays in conditions that directly mimic the protein, nucleotide, and caged-nucleotide concentrations present in the infrared films. However, we can determine PGK activity in concentrations of buffer salts that are similar to those found in the infrared samples.

Table 1: PGK Activity Assays[a]

[ATP] (mM)	control (s^{-1})	+NPE-ATP (s^{-1})	+NPE-ADP (s^{-1})
0.025	75	74	20
0.05	96	80	40
0.25	157	143	67

[a] Rates are averages of three activity assays performed on PGK in buffer M given in mol product/mol PGK s. Concentrations as described in Materials and Methods.

In order to ensure that PGK is still active in the high concentrations of buffer salts that are present in infrared samples, activity assays were performed in 100× buffer M (*26*). The high salt activity assays indicated that the PGK had rates of approximately 25% of the original activity observed in buffer M, yet the PGK was still able to perform the phospho-transfer reaction. Additional activity assays were performed in variations of 100× buffer M in order to determine the buffer component that was responsible for the decreased rates. Activity assays were performed in multiple buffers that contained 100× concentrations of each of the original buffer M components (HEPES, EDTA, $MgCl_2$, and DTT) while buffer M concentrations of the other three components were maintained. The results of these additional assays suggest that the high HEPES concentrations are responsible for the decreased activity observed in the 100× buffer M activity assays (data not shown). Previous studies have suggested that sulfate ions can interfere with substrate binding and decrease enzyme activity (*2*, *25*, *29*). Therefore, it is likely that high concentrations of HEPES may interfere with substrate binding. It should be noted that PGK−3-PG samples start at low HEPES concentrations (20 mM), where the 3-PG is most likely initially bound to the enzyme, but the buffer concentrations will gradually increase as partial dehydration occurs.

Difference Infrared Spectra. Light-minus-dark difference spectra obtained on various PGK samples were generated by taking a ratio of a spectrum taken after photolysis to one taken before photolysis. The averaged light-minus-dark spectra obtained in the absence of protein were normalized for photolytic release and then subtracted from the averaged difference spectra taken in the presence of protein. The following difference spectra were generated and are shown in Figures 2−4: PGK−ATP minus PGK, PGK−ADP minus PGK, PGK−ATP−3-PG minus PGK−3-PG, and PGK−ADP−3-PG minus PGK−3-PG. Individual samples that contained a 4:1 to 10:1 ratio of caged-nucleotide to protein yielded similar difference spectra. Figures 2−4 display the 1800−1300 cm^{-1} region that includes the amide I region

(~1690−1620 cm^{-1}) and the amide II region (~1550 cm^{-1}) that are dependent on the secondary structure of the protein (*30*). Other bands observed throughout the 1800−1300 cm^{-1} region are associated with specific amino acid side chains and any nucleotide vibrations that are perturbed upon binding (*31*, *32*). Unpublished absorbance spectra of 3-PG show that most bands are below 1300 cm^{-1}, but there is a very small (compared to nucleotide) broad absorbance around 1600 cm^{-1}. The numerous signals present in Figures 2−4 indicate that a variety secondary structures and amino acid side chains are differentially influenced by ADP and ATP binding to PGK.

Comparison of ATP and ADP Binding to PGK and PGK−3-PG. The comparison of difference spectra associated with ATP and ADP binding to PGK in the absence of 3-PG show similar band intensities but a number of different absorptions (Figure 2, top section). The differences in the 1690−1600 cm^{-1} region could be associated with protein secondary structural changes induced by ADP and ATP binding. The difference infrared data only reflect the net changes in structure. The PGK−ATP difference data are more complex in the 1645−1695 cm^{-1} region. For example, the positive 1651 cm^{-1} vibration that is more intense in the PGK−ATP complex, as compared to the PGK−ADP complex, could arise from a change in the α-helix that is specific to the PGK−ATP conformation (*30*). Some other bands that show greater intensity in the PGK−ATP complex, as compared to the PGK−ADP complex, include positive 1620 and 1637 cm^{-1} bands and negative intensity around 1645 and 1679 cm^{-1}. The PGK−ADP minus PGK difference data contain more negative intensity around 1660 cm^{-1} as compared to the PGK−ATP minus PGK data.

Comparison of ADP and ATP binding to the PGK−3-PG complexes shows some of the same variations observed in the binary complexes (around 1685, 1670, 1645, and 1630 cm^{-1}) and additional differences between the two spectra associated with the ternary complexes (Figure 2, bottom panel). The activity assays suggest that caged-ADP (not caged-ATP) may be interacting with the substrate(s) binding sites. If similar interactions occur under protein and nucleotide concentrations found in the infrared samples, the differences between ATP and ADP binding to PGK and PGK−3-PG complexes could originate from different interactions between the caged-complexes and PGK. Other differences may be due to the two possible binding sites for the phosphate chain on the ATP (*10*). ATP has a more flexible phosphate chain that can switch between two binding sites within the active site (*10*). Unfortunately, we cannot definitively assign the differences observed between the two nucleotides. However, additional information may be obtained by comparing the binding of each nucleotide to PGK and PGK−3-PG complexes and from studying infrared data obtained from the nucleotide exchange experiments (Figure 5).

Comparison of ADP binding to PGK and PGK−3-PG. Figure 3 shows the difference spectra associated with ADP binding to PGK and PGK−3-PG complexes. The difference spectra presented in Figure 3 show similar intensity and band positions with a few small differences observed between the binary and ternary complexes. The overall similarity between the two difference spectra suggests that analogous changes in secondary structures are associated with ADP binding to PGK and the PGK−3-PG complex. The 1620−1695 cm^{-1} region of the spectra are similar and suggest that the major changes in PGK secondary structure that occur upon ADP release and binding are not greatly influenced by the presence of 3-PG. There are small negative intensities only associated with the ternary complex (Figure 3, dashed line) that are around 1674, 1633, 1624, 1606, 1570, and 1468 cm^{-1}. Arg (1673 cm^{-1}), Asn (1678 cm^{-1}), and Gln (1668−1687 cm^{-1}) all have bands near 1674 cm^{-1} (*31*, *33*). Lys, Arg, and His have bands around 1626−1636 cm^{-1}, while Gln (1586−1610 cm^{-1}) and Phe (1585 and 1605 cm^{-1}) are both possible contributors to the 1581 and 1606 bands (*26*, *31*, *33*). Asp and Glu vibrations occur in the 1560−1580 and 1400 cm^{-1} region, while Phe, Pro, and His are all candidates for the 1450−1470 cm^{-1} bands (*31*, *33*). The increased stabilization of the PGK−ADP−3-PG complex as observed in protein unfolding experiments suggests that the small differences between the spectra in Figure 3 may arise from important stabilizing interactions between the two domains (*4*). Most of the distinctive bands in the PGK−ADP−3-PG complex could be explained by the formation or perturbation of salt bridges between domains. Another possibility is that the presence of the caged-ADP in the samples prevents proper 3-PG binding until after the ADP is released from its caged-complex.

Comparison of ATP Binding to PGK and PGK−3-PG. Figure 4 shows the difference infrared spectra associated with ATP binding to PGK and PGK−3-PG complexes. The comparison of the difference spectra associated with the binary and ternary complexes shows substantial differences throughout the 1800−1300 cm^{-1} region. The PGK−ATP−3-PG data (Figure 4, dashed line) have decreased intensities throughout the region (as compared to PGK−ATP data, Figure 4 solid line) and a significant decrease in intensity around 1637 cm^{-1}. The wider linewidths and decreased intensity of some of the bands in the PGK−ATP−3-PG spectra may arise from a more diverse set of PGK structures. Differences in intensity around 1625−1640 and 1675−1695 cm^{-1} may be due to altered β-sheet structures (*30*). More negative bands around 1686 and 1672 cm^{-1} are only found the PGK−ATP−3-PG difference data (Figure 4, dashed line). Bands in this region can be associated with changes in β-structure or amino acid side chains such as Asn, Gln, and Arg (*30*, *31*, *33*). Vibrations associated with the PGK−ATP−3-PG ternary complexes occur around 1672, 1637, 1620, 1609, 1566, and 1468 cm^{-1} (Figure 4) and are similar to those identified in the PGK−ADP−3-PG complexes (Figure 3). We observe additional decreases in intensities around 1470−1450 and 1410−1380 cm^{-1} in the PGK−ATP−3-PG data when compared to the PGK−ATP data (Figure 4). The PGK−ATP−3-PG difference spectrum also contains positive bands around 1705, 1680, 1535, and 1510−1490 cm^{-1} (Figure 4, dashed line). Asp and Glu (COOH) vibrations may occur in the 1760−1710 cm^{-1} region (*31*, *33*). A peak associated with ATP binding to PGK−3-PG complexes was observed at 1535 cm^{-1} and could be due to perturbations in a Lys side chain (*22*). Pro, Trp, and Asn side chains all have infrared absorbances around 1620 cm^{-1}, and Asp and Glu (COO−) vibrations are observed around 1560−1580 and ~1400 cm^{-1} (*31*, *33*, *34*). Difference data associated with each of the ternary complexes show decreased intensity around 1570 cm^{-1}. However, the data associated with the

Table 2: Unique Infrared Signals Associated with PGK−ATP−3-PG Complexes

PGK−ATP−3-PG bands		
Figure 4	Figure 5	tentative assignments
(+) 1730−1705	(+) 1730−1705	Asp, Glu (COOH)
(−) 1686	(−) 1686	*β*, Gln
(+) 1681	(−) 1678	*β*, Asn, Gln, Arg
(−) 1672		Asn/Gln/Arg
(+) 1661	(+) 1661	α-helix, nucleotide
(−) 1651		α-helix, nucleotide
(−) 1637	(−) 1637	*β*, Arg, Lys
(−) 1624	(+) 1628	*β*, Lys,His
	(+) 1620	*β*, Tyr, Trp, Pro
(−) 1614		Gln, Tyr, Asn, Pro
	(+) 1603	nucleotide/Tyr/Phe
(−) 1566		Asp, Glu (COO^-)
(+) 1535		Lys
(+) 1502		Tyr, Phe, Trp
	(+) 1485−1430	Phe, Pro, Trp, His, Thr
(−) 1397		Pro, Trp, Asp, Glu, Thr
	(−) 1340	nucleotide, Trp

PGK−ATP−3-PG complex compared to the PGK−ADP−3-PG complex has a broader, more intense difference in this region and may suggest the participation of multiple Asp and Glu side chains in the formation of the active complex. Other candidates for the differences observed around 1398 cm^{-1} could include Pro (1400−1465 cm^{-1}), Trp (1412−1435 cm^{-1}), or Thr (1385−1420). Glu341, Asp372, Pro336, Lys213, and Lys217 are all located in the nucleotide binding site and could account for some of the vibrational differences we observe (*2*). Figure 4 also shows that some bands are only found in the PGK−ATP minus PGK difference spectra and include positive bands at 1620, 1579, and ca. 1398 cm^{-1}.

Nucleotide Exchange. The results of the activity assays in buffer M suggest that the caged-ADP and caged-ATP may interact differently with PGK in more dilute protein and nucleotide concentrations than those found in the infrared films. The possibility exists that the comparison of the PGK−ATP minus PGK and PGK−ADP minus PGK difference data obtained in Figures 2−4 may also include some variation between the initial PGK−caged-nucleotide complexes. In order to provide an additional means to identify bands associated with each of the PGK−nucleotide bound states, we performed infrared experiments where PGK−ADP complexes were exchanged with excess ATP released from the caged-complex. In these experiments, the caged-ATP should not interact with the PGK until it is released from its cage and subsequently displaces the ADP from PGK. The $MgCl_2$ used in buffer M ensures Mg^{2+} is present in the infrared samples and results in Mg−nucleotide−PGK complexes. The excess ATP (10:1 ratio of ATP:PGK) should ensure nucleotide exchange. In addition, the nature of difference infrared spectroscopy dictates that only the proteins that exchange nucleotides (or change after photolytic release of caged-ATP) will contribute to the difference infrared spectra observed in Figure 5. The difference spectra shown (Figure 5, solid line) reflect those changes that result from the displacement of ADP and binding of ATP in the absence of 3-PG.

Previous studies have shown that PGK−ATP and PGK−ADP complexes are quite different from each other and that the PGK−ADP structure is a more stable structure (*4*, *10*, *35*). Additional studies have suggested that the MgATP

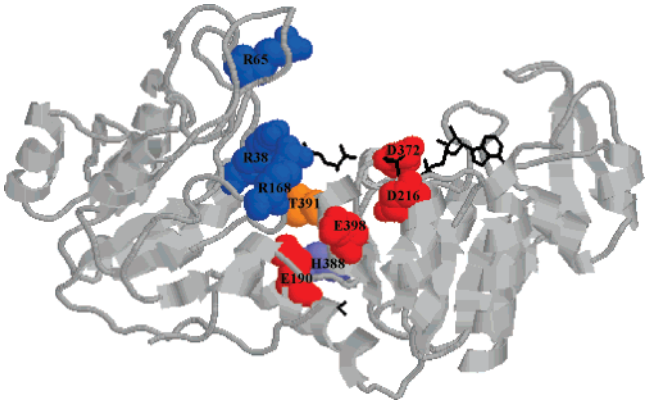

FIGURE 6: The open structure of yeast PGK with some examples of amino acids that could be involved in ternary complex formation and domain closure shown in spacefill (*2*, *4*−*7*).

structure has greater flexibility due to two possible terminal phosphate binding sites for ATP (*10*). Evidence for differential binding also comes from studies performed on human PGK Lys215 mutants. This substitution weakens the MgATP binding but not the MgADP binding (*36*). The mutation studies agree with the *T. brucei* crystal structure that shows that the Mg^{2+} is not directly coordinated to the protein in the PGK−AMP−PNP complex, as is observed in the MgADP complex (*9*). Equilibrium dialysis and NMR studies have also shown different locations for the cation in each of the nucleotide complexes and tighter MgADP binding to PGK (*28*, *35*). These differences should be reflected in Figure 5 (solid line).

In the absence of 3-PG, the difference data associated with PGK−ATP minus PGK−ADP show positive 1651 and 1637 cm^{-1} bands and negative signals at 1695, 1662, and 1645 cm^{-1} that are most likely associated with some secondary structures that are differentially influenced by nucleotide binding. When ATP is bound, there is a change in the α-helix shown by the negative 1662 and 1645 cm^{-1} peaks and a possible increase in *β*-structure, as shown by the positive 1637 cm^{-1} peak (*30*). The intensity at 1637 cm^{-1} could also arise from Arg or Lys side chains. Changes around 1580 and 1400 cm^{-1} may be due to the COO^- vibrations of Asp or Glu that are altered upon nucleotide exchange (*31*). A positive peak at 1446 cm^{-1} could be associated with a Pro perturbation such as the Pro 336 in the nucleotide binding site (*31*). Further insight into the differences between ATP and ADP binding can be observed in the inset. The inset shows an overlay of the PGK−ATP minus PGK−ADP exchange spectrum (Figure 5, solid line) with another spectrum (dashed line) obtained by subtracting PGK−ADP (Figure 2, dashed line top) from PGK−ATP spectrum (Figure 2, solid line top). Although both spectra shown in the inset should reflect differences between ADP and ATP binding, the magnitude of the peaks differs by about a factor of 5. It is possible that the inset provides additional evidence that the original PGK−caged-nucleotide interactions are different for caged-ATP and caged-ADP. Another possible explanation for the inset is that the initial nucleotide binding causes the largest changes and that the exchange data only include differences arising from the terminal phosphate on ATP and the corresponding rearrangements in protein structure.

Nucleotide exchange experiments were also performed in the presence of 3-PG in order to investigate how the different

nucleotides influence the ternary complex. Many of the changes observed in the presence of 3-PG (Figure 5, dashed line) are similar to those observed in its absence (Figure 5, solid line). However, numerous additional changes are also observed when PGK−ADP−3-PG complexes exchange ADP for ATP. Positive peaks around 1730−1720 and at 1705 cm^{-1} may arise from Asp or Glu (COOH) residues influenced by ATP binding. A large positive 1651 cm^{-1} vibration suggests that a unique change in α-helix is associated with the active, ATP ternary complex (*30*, *31*). In addition, there is an increase of negative intensity in the 1690−1675 cm^{-1} region that could also reflect a perturbation in side chains such as Arg, Asn, and Gln as well as altered β-structure (*30*, *31*). Similarly, a broad positive feature from 1630 to 1600 cm^{-1} is unique to the nucleotide exchange in the ternary complex and could contain contributions from β-sheet or side chains such as Lys or Arg (*30*, *31*). The small positive peak around 1535 cm^{-1} is also suggestive of a Lys side chain that reorients upon ATP exchange (*31*, *33*). Perhaps the most pronounced differences associated with the ternary complex exchange occur in the 1510−1430 cm^{-1} region. Many of these bands could be associated with amino acids, such as Phe, Trp, and Pro side chains (*31*, *33*). The intensity of the positive peaks in this region suggests that numerous side chains are perturbed when ATP is substituted for ADP in the ternary complex. What is interesting is the similar intensity around 1400 cm^{-1} that suggests that the Asp and Glu (COO^-) side chains influenced by nucleotide exchange are not differentially altered when 3-PG is present in the complex (*31*). However, other Asp and Glu residues (COOH) are uniquely influenced by nucleotide exchange in the 3-PG complex, as evidenced by the positive intensity in the 1730−1700 cm^{-1} region (*31*, *33*). These bands may be associated with the productive, most closed, PGK ternary complex. Varga et. al have suggested that side-chain hydrogen bonding and electrostatic interactions between Asp and Glu residues as well as Lys and Arg are crucial for the formation of the closed PGK structure (*4*).

CONCLUSIONS

We have presented the first difference infrared studies of nucleotide binding to PGK. The difference infrared data provide complementary information to that previously obtained using other spectroscopic techniques. The sample conditions used to generate the difference infrared data most likely have high concentrations of buffer salts and could be somewhat similar to crystal conditions with high sulfate concentrations (*2*). However, the partially dehydrated infrared samples resemble thin films and may exist in a more gel-like intermediary state between solution and crystal conditions. The ability to directly compare data associated with each of the complexes has allowed us to isolate important signals that are associated with each of the PGK ternary complexes. Changes that would be specific to 3-PG binding that are not influenced by nucleotide binding would be subtracted out using our methods, as the 3-PG is always bound to PGK before the nucleotides are released. We are not able to perform an experiment where we would initiate 3-PG binding externally, as caged-3-PG is not commercially available. Previous DSC studies suggest that 3-PG binding to PGK may show even larger changes as 3-PG binding stabilizes PGK more than MgATP or MgADP binding (*4*). The similarities of bands observed in difference data associated with the ternary complexes suggest some comparable interactions between side chains for both PGK−ADP−3-PG and PGK−ATP−3-PG complexes. Our data support the fact that additional interactions present in both ternary complexes arise from new salt bridges and the movement of helices, sheets, and other protein structures as a result of domain closure. Interactions between domains have been proposed by Varga et al. and include new hydrogen-bonding and electrostatic interactions between residues such as arginine, threonine, lysine, asparagine, aspartate, glutamate, and histidine (*4*, *5*).

Comparison of the data in Figures 4 and 5 also shows signals that are only associated with the productive PGK−ATP−3-PG complex. These bands could prove to be the most interesting. Although we cannot definitively say whether the PGK adopts a closed conformation, we can discern substantial differences between the PGK−ATP and PGK−ATP−3-PG complexes. Our data support previous studies on human PGK ternary complexes and suggest that the yeast PGK−ATP−3-PG complexes may exist in a more compact state than the PGK−ADP−3-PG complexes (*5*). Table 2 summarizes the bands that are associated with the productive ternary complex and suggests some tentative assignments for these interesting peaks. Figure 6 shows the yeast PGK structure with some of the amino acids that may be involved in domain closure (*2*, *4*−*7*). Many of the infrared bands that are associated with the active ternary complex are consistent with the formation of salt-bridges and alternate secondary structures necessary for phospho-transfer (Table 2).

The most interesting peaks should be those that are found only in the PGK−ATP−3-PG difference data and are also observed in the PGK−ATP−3-PG exchange data (Table 2). Numerous bands support the involvement of lysine and arginine side chains in the productive complex. Figures 4 and 5 show changes in the 1637 cm^{-1} peak when the PGK−ATP−3-PG spectra are compared to either the PGK−ATP or PGK−ADP−3-PG spectra. The difference in intensity may be due to an Arg that is differently influenced by the PGK−ATP−3-PG complex (*31*). For example, the crystal structure of 3-PG bound to pig muscle PGK shows that there is an H bond between an arginine and a threonine (*3*, *4*). Another vibration that may be assigned to a perturbation of an Arg is around 1680 cm^{-1}. For the interdomain contacts to occur between a positively charged side chain of the Arg or Lys, there should be a negatively charged side chain in the other domain that participates in the formation of new contact (Figure 6). We expect that the negative charge may arise from a COO− on either an Asp or a Glu side chain that would appear in the 1580−1560 and 1400 cm^- regions (*31*). In all cases where the binary and ternary complexes are compared, we observe some changes in these regions. Difference data associated with each of the ternary complexes show decreased intensity around 1570 cm^{-1}. However, the data associated with the PGK−ATP−3-PG complex shows a broader, more intense difference in this region and may suggest participation of multiple Asp and Glu side chains in the formation of the active complex. The changes that are reproducibly unique to the PGK−ATP−3-PG complex are consistent with the formation of new hydrogen-bonding interactions between side chains from different domains and

the movement of both β-structure and α-helices around the nucleotide binding sites and in the hinge region.

REFERENCES

1. Banks, R. D., Blake, C. C. F., Evans, P. R., Haser, R., Rice, D. W., Hardy, G. W., Merrett, M., and Phillips, A. W. (1979) Sequence, structure and activity of phophoglycerate kinase: A possible hinge-bending enzyme, *Nature 279*, 773−777.
2. Watson, H. C., Walker, N. P. C., Shaw, P. J., Bryant, T. N., Wendell, P. L., Fothergill, L. A., Perkins, R. E., Conroy, S. C., Dobson, M. J., Tuite, M. F., Kingsman, A. J., and Kingsman, S. M. (1982) Sequence and structure of yeast phosphoglycerate kinase, *EMBO J. 1*, 1635−1640.
3. Szilagyi, A. N., Ghosh, M., Garman, E., and Vas, M. (2001) A 1.8 A resolution structure of pig muscle 3-phosphoglycerate kinase with bound MgADP and 3-phosphoglycerate in open conformation: New insight into the role of the nucleotide in domain closure, *J. Mol. Biol. 306*, 499−511.
4. Varga, A., Flachner, B., Graczer, E., Osvath, S., Szilagyi, A. N., and Vas, M. (2005) Correlation between conformational stability of the ternary enzyme−substrate complex and domain closure of 3-phosphoglycerate kinase, *FEBS J. 272*, 1867−1885.
5. Varga, A., Flachner, B., Konarev, P., Graczer, E., Szabo, J., Svergun, D., Zavodszky, P., and Vas, M. (2006) Substrate-induced double sided H-bond network as a means of domain closure in 3-phosphoglycerate kinase, *FEBS Lett. 580*, 2698−2706.
6. Auerbach, G., Huber, R., Grattinger, M., Zaiss, K., Schurig, H., Jaenicke, R., and Jacob, U. (1997) Closed structure of phosphoglycerate kinase from *Thermotoga maritima* reveals the catalytic mechanism and determinants of thermal stability, *Structure 5*, 1475−1483.
7. Lee, J. H., Im, Y. J., Bae, J., Kim, D., Kim, M.-K., Kang, G. B., Lee, D.-S., and Eom, S. H. (2006) Crystal structure of *Thermus caldophilus* phosphoglycerate kinase in the open conformation, *Biochem. Biophys. Res. Commun. 350*, 1044−1049.
8. Bernstein, B. E., Michels, P. A. M., and Hol, W. G. J. (1997) Synergistic effects of substrate-induced conformational changes in phosphoglycerate kinse activation, *Nature 385*, 275−278.
9. Bernstein, B. E., and Hol, W. G. J. (1998) Crystal structures of substrates and products bound to the phosphoglycerate kinase active site reveal the catalytic mechanism, *Biochemistry 37*, 4429−4436.
10. Flachner, B., Kovari, Z., Varga, A., Gugolya, Z., Vonderviszt, F., Naray-Szabo, G., and Vas, M. (2004) Role of phosphate chain mobility of MgATP in completing the 3-phosphoglycerate kinase catalytic site: Binding, kinetic, and crystallographic studies with ATP and MgATP, *Biochemistry 43*, 3436−3449.
11. Kovari, Z., Flachner, B., Naray-Szabo, G., and Vas, M. (2002) Crystallographic and thiol-reactivity studies on the complex of pig muscle phosphoglycerate kinase with ATP analogues: Correlation between nucleotide binding mode and helix flexibility, *Biochemistry 41*, 8796−8806.
12. Kovari, Z., and Vas, M. (2004) Protein conformer selection by sequence-dependent packing contacts in crystals of 3-phosphoglycerate kinase, *Proteins 55*, 198−209.
13. May, A., Vas, M., Harlos, K., and Blake, C. (1996) 2.0 Å Resolution structure of a ternary complex of pig muscle phosphoglycerate kinase containing 3-phospho-D-glycerate and the nucleotide Mn adenylylimidodiphosphate, *Proteins 24*, 292−303.
14. Harlos, K., Vas, M., and Blake, C. F. (1992) Crystal Structure of the binary complex of pig muscle phosphoglycerate kinse and its substrate 3-phosphoglycerate, *Proteins 12*, 133−144.
15. Joao, H. C., and Williams, R. J. P. (1993) The anatomy of a kinase and the control of phosphate transfer, *Eur. J. Biochem. 216*, 1−18.
16. Wilson, H. R., Williams, R. J. P., Littlechild, J. A., and Watson, H. C. (1988) NMR analysis of the interdomain region of yeast phosphoglycerate kinase, *Eur. J. Biochem. 170*, 529−538.
17. Tanswell, P., Westhead, E. W., and Williams, R. J. P. (1976) Nuclear-magnetic-resonance study of the active-site structure of yeast phosphoglycerate kinase, *Eur. J. Biochem. 63*, 249−262.
18. Fairbrother, W. J., Graham, H. C., and Williams, R. J. P. (1990) An NMR study of anion binding to yeast phosphoglycerate kinase, *Eur. J. Biochem. 190*, 161−169.
19. Fairbrother, W. J., Walker, P. A., Minard, P., Littlechild, J. A., Watson, H. C., and Williams, R. J. P. (1989) NMR analysis of site-specific mutants of yeast phosphoglycerate kinase: An investigation of the triose-binding site, *Eur. J. Biochem. 183*, 57−67.
20. Sherman, M. A., Fairbrother, W. J., and Mas, M. T. (1992) Characterization of the structure and properties of the His62→Ala and Arg38→Ala mutants of yeast phosphoglycerate kinase: An investigation of the catalytic and activatory sites by site-directed mutagenesis and NMR, *Protein Sci. 1*, 752−760.
21. Pickover, C. A., McKay, D. B., Engelman, D. M., and Steitz, T. A. (1979) Substrate binding closes the cleft between the domains of yeast phosphoglycerate kinase, *J. Biol. Chem. 254*, 11323−11329.
22. Barth, A., and Zscherp, C. (2002) What vibrations tell us about proteins, *Q. Rev. Biophys. 35*, 369−430.
23. Barth, A., and Zscherp, C. (2000) Substrate binding and enzyme function investigated by infrared spectroscopy, *FEBS Lett. 477*, 151−156.
24. Pace, C. N., Vajdos, F., Fee, L., Grimsley, G., and Gray, T. (1995) How to measure and predict the molar absorption coefficient of a protein, *Protein Sci. 4*, 2411−2423.
25. Scopes, R. K. (1978) The steady-state kinetics of yeast phosphoglycerate kinase: Anomalous kinetic plots and the effects of salts on activity, *Eur. J. Biochem. 85*, 503−516.
26. Schwartz, C. M., Drown, P. M., and MacDonald, G. (2005) Difference FTIR studies reveal nitrogen-containing amino acid side chains are involved in the allosteric regulation of RecA, *Biochemistry 44*, 9733−9745.
27. Barth, A., Mantele, W., and Kreutz, W. (1991) Infrared spectroscopic signals arising from ligand binding and conformational changes in the catalytic cycle of sarcoplasmic reticulum calcium ATPase, *Biochim. Biophys. Acta 1057*, 115−123.
28. Molnar, M., and Vas, M. (1993) Mg^{2+} affects the binding of ADP but not ATP to 3-phosphoglycerate kinase: Correlation between equilibrium dialysis binding and enyme kinetic data, *Biochem. J. 293*, 595−599.
29. Larsson-Raznikiewicz, M., and Jansson, J. R. (1973) Activation of yeast phosphoglycerate kinase by salts of monovalent cations, *FEBS Lett. 29*, 345−347.
30. Jackson, M., and Mantsch, H. H. (1995) The use and misuse of FTIR spectroscopy in the determination of protein structure, *Crit. Rev. Biochem. Mol. Biol. 30*, 95−120.
31. Barth, A. (2000) The infrared absorption of amino acid side chains, *Prog. Biophys. Mol. Biol. 74*, 141−173.
32. El-Mahdaoui, L., and Tajmir-Riahi, H. A. (1995) A comparative study of ATP and GTP complexation with trivalent Al, Ga and Fe cations. Determination of cation binding site and nucleotide conformation by FTIR difference spectroscopy, *J. Biomol. Struct. Dyn. 13*, 69−86.
33. Venyaminov, S. Y., and Kalnin, N. N. (1990) Quantitative IR spectrophotometry of peptide compounds in water (H_2O) solutions. I. Spectral parameters of amino acid residue absorption bands, *Biopolymers 30*, 1243−1257.
34. Gerwert, K., Hess, B., and Englehard, M. (1990) Proline residues undergo structural changes during proton pumping in bacteriorhodopsin, *FEBS Lett. 261*, 449−454.
35. Raghunathan, V., Chau, M. H., Ray, B. D., and Rao, B. D. N. (1999) Structural characterization of manganese(II)−nucleotide complexes bound to yeast 3-phosphoglycerate kinase: ^{13}C relaxation measurements using [U-^{13}C]ATP and [U-^{13}C]ADP, *Biochemistry 38*, 15597−15605.
36. Flachner, B., Varga, A., Szabo, J., Barna, L., Hajdu, I., Gyimesi, G., Zavodszky, P., and Vas, M. (2005) Substrate-assisted movement of the catalytic Lys 215 during domain closure: Site-directed mutagenesis studies of human 3-phosphoglycerate kinase, *Biochemistry 44*, 16853−16865.

BI701723C